REPORT DOCUMENTATION PAGE

Form Approved
OMB NO. 0704-0188

Public Reporting burden for this collection of information is estimated to average 1 hour per response, including the time for reviewing instructions, searching existing data sources, gathering and maintaining the data needed, and completing and reviewing the collection of information. Send comment regarding this burden estimates or any other aspect of this collection of information, including suggestions for reducing this burden, to Washington Headquarters Services, Directorate for information Operations and Reports, 1215 Jefferson Davis Highway, Suite 1204, Arlington, VA 22202-4302, and to the Office of Management and Budget, Paperwork Reduction Project (0704-0188,) Washington, DC 20503.

1. AGENCY USE ONLY (Leave Blank)	2. REPORT DATE June 26, 2003	3. REPORT TYPE AND DATES COVERED Final Report April 1 2001 – March 31, 2003

4. TITLE AND SUBTITLE Acquisition of a Small Angle X-ray Scattering (SAXS) System for the Study of Nanostructured Materials	5. FUNDING NUMBERS N00014-01-1-0613
6. AUTHOR(S) E.J. Lavernia	

7. PERFORMING ORGANIZATION NAME(S) AND ADDRESS(ES) University of California, Irvine 160 Administration Building Irvine, CA 92697	8. PERFORMING ORGANIZATION REPORT NUMBER

9. SPONSORING / MONITORING AGENCY NAME(S) AND ADDRESS(ES) Office of Naval Research 800 North Quincy Street Arlington, VA 22217-5660	**20030801 176**

11. SUPPLEMENTARY NOTES

The views, opinions and/or findings contained in this report are those of the author(s) and should not be construed as an official Department of the Army position, policy or decision, unless so designated by other documentation.

12 a. DISTRIBUTION / AVAILABILITY STATEMENT Approved for public release; distribution unlimited.	12 b. DISTRIBUTION CODE

13. ABSTRACT (Maximum 200 words)

A NanoSTAR small angle X-ray scattering (SAXS) system (Manufacturer: Bruker AXS, Inc.) was acquired in support of research on nanostructured materials. A unique feature of the acquired instrument is its capability for materials characterization on a nanometer length scale. Research programs that uniquely benefit from the acquired equipment involve the processing and synthesis of bulk nanostructured materials by consolidation and direct fabrication methods, as well as nanostructured coatings. In-depth understanding of the relevant fundamental phenomena is necessary, for example, effects of dispersoids on the grain growth in nanostructured materials, in order to fully exploit the potential of nanostructured materials. In the case of crystalline substances, SAXS studies are aimed at determining the scattering intensity near the origin of the reciprocal lattice of the substances. Contrary to the determination of atomic structure by the X-ray diffractometer (XRD), SAXS is used to identify the disturbances in this structure, providing information about the orientation, the form, and the order of magnitude of the defects, the characteristic sizes of dispersoids, precipitates or pores/voids in the crystal, phase formation resulting from aging, annealing and heating, and others. Under this program, the following accomplishments have been achieved: (1) The acquired SAXS system was successfully installed and is now in operational condition; a short training course was provide to graduate students and faculty; (2) method for interpretation of experimental SAXS data was developed using Mathematica Analysis; (3) lattice spacing at a large scale was determined using the SAXS; (4) interface between ceramic and metal was characterized, in particular in interface geometry and defects; (5) crystalline phase size distributed in amorphous matrix was analyzed; and (6) crystallization behavior was investigated in combination with DSC and TEM.

14. SUBJECT TERMS Small Angle X-ray Scattering (SAXS), nanocrystalline powders, interface, dispersoids, and amorphous phase		15. NUMBER OF PAGES
		16. PRICE CODE

17. SECURITY CLASSIFICATION OR REPORT **UNCLASSIFIED**	18. SECURITY CLASSIFICATION ON THIS PAGE **UNCLASSIFIED**	19. SECURITY CLASSIFICATION OF ABSTRACT **UNCLASSIFIED**	20. LIMITATION OF ABSTRACT **UL**

NSN 7540-01-280-5500

Standard Form 298 (Rev.2-89)
Prescribed by ANSI Std. 239-18
298-102

1. Scientific Personnel

Kit Foo, Ph.D. student
Zhihui Zhang, Ph.D. student
Alejandro Zuniga, PhD student
Dr. Yizhang Zhou, Associate Researcher
Darryl Mack, Associate Development Engineer

2. Acquired Instrument

The acquired instrument is the NanoSTAR small angle X-ray scattering (SAXS) system equipped with a GGCS goniometer control system and HiStar detector, manufactured by Bruker AXS, Inc. The unique feature of the instrument is its capability for characterization on a nanometer length scale in the range of 10 Angstroms up to 10^4 Angstroms. The complete SAXS system is an integrated unit primarily comprised of the SAXS area detector system, high resolution X-ray small angle pin hole chamber (HR-PHK), NanoStar X-ray benchtop (rack and X-ray generator), general goniometer control system (GGCS), HiStar detector, DIFFRAC^{plus} software, cross coupled Göbel mirrors for Cu radiation, and accessories.

The HR-PHK chamber is designed for the NanoStar system. The incident beam for doing SAXS with the HR-PHK is conditioned by a sealed tube and cross coupled Göbel Mirrors. The SAXS signals are collected with the HiStar detector. The NanoStar X-ray benchtop is the working station for the NanoStar system. It is a base cabinet rack carrying the X-ray generator Kristalloflex, the GGCS motor controller and interlock controller, and other optional equipment like an internal water chiller. The X-ray generator Kristalloflex is microprocessor-controlled, solid state, medium frequency, X-ray generator for a maximum power of 3.0 kW. The single shutter tube housing is screwed on a mount with several degrees of freedoms to ensure that the beam defined by the X-ray source and the cross coupled Göbel Mirrors can be aligned with respect to the pin hole chamber HR-PHK. The SAXS area detector system is used for frame data acquisition and imaging with high stability, high throughout, and high resolution. It features selectable 1024x1024 or 512x512 pixel frames.

The GADDS software for SAXS is a frame buffer software for data collection, display, and reduction, including real-time data collection on VGA color display. It can also control a sample stage/changer so that multiple samples or different regions of the same sample can be investigated without removing the sample from the vacuum. The DIFFRAC^{plus} TOPAS is the most efficient analysis software available. It can generate profiles fitting of individual or multiple, overlapping diffraction peaks. This software provides automatic or interactive handling of peak parameters for position, background, width, height, and shape exponents for the profile function. Also, it provides output of refined parameters for peak position, Full Width Half Maximum (FWHM), peak height, peak integrated area, and profile exponents. The DIFFRAC^{plus} TOPAS software has the power to select the crystallographic phases, and the search criteria, such as database selection, as well as optional input of chemical constraints. It provides easy simulation and automatic refinement of measured data, fast 3D graphics and full integration into the Window environment.

Another important feature of the instrument is the cross coupled Göbel Mirrors for Cu radiation. The assembly works as a dispersive X-ray optical component which separates Cu-Kα radiation from Cu-Kβ and the continuum. It provides a highly intense parallel X-ray beam with a small cross section, which means high brilliance. The primary advantage of the assembly is the significant intensity gain, compared to other assembly such as graphite monochromator/collimator. The cross coupled Göbel Mirrors enhance the useful solid angle of X-rays emitted by the tube, resulting in a higher angular resolution of X-ray beam. The smaller the required beam size, the higher the intensity gain is. Typically, the Göbel Mirrors give more primary beam intensity if the required beam size is below 0.5 mm, as in the case of small angle X-ray scattering with high resolution and residual stress and texture investigations.

3. Scientific Progress and Accomplishments

This program was to acquire a small angle X-ray scattering (SAXS) system, and to utilize the acquired SAXS system for fundamental studies in association with development of nanostructured materials. Under this program, the following accomplishments have been achieved: (1) The acquired SAXS system was successfully installed and is now in operational condition; a short training course was provide to graduate students and faculty; (2) methods for interpretation of experimental SAXS data was developed using Mathematica Analysis; (3) lattice spacing at a large scale was determined using the SAXS; (4) interface between ceramic and metal was characterized, in particular in interface geometry and nano-voids; (5) crystalline phase size distributed in amorphous matrix was analyzed; and (6) crystallization behavior was investigated in combination with DSC

and TEM. This final report covers the progress made during the period from April 01, 2001 – March 31, 2003. The primary research accomplishments are briefly summarized as follows.

3.1. Large d-spacing measurement

The SAXS can be used to determine the d-spacing up to tens of nanometers; whereas for a conventional XRD, the measurement is done in the range of several Angstroms. If the scattering angle is too small ($2\theta < 2°$), the background scattering becomes significant and thus makes it difficult to distinguish the Bragg peaks from the background. Figure 1 shows the XRD patterns for a quartz plate in the range of 1~100° performed on a Scintag XDS 2000 X-ray Diffractometer using CuK$_\alpha$ radiation. The quartz single crystal is cut 6° from (0001) and such an orientation contributes no Bragg peaks due to diffraction. However, one can see a sharp peak may occur at very small angles and the background intensity drops to below 50 CPS when $2\theta > 2°$. Figure 2 shows the scattering pattern for a carboxylate of silver behenate, CH3(CH2)20COOAg, whose (0 0 l) long-period spacing of 58.38 Å could be easily determined by measuring the diameter of the diffraction ring in the reciprocal space. The characteristic dimension D that can be measured by the SAXS could be estimated as:

Figure 1. XRD pattern for a quartz single crystal cut 6° from (0001) showing the background noise at very small angles.

$$D = \frac{2\pi}{q}, \quad where \quad q = \frac{4\pi \sin\theta}{\lambda}$$

Hence the d-spacing in the range of 3 ~ 63 nm could be measured on the Bruker-AXS NanoStar instrument, corresponding to 0.14 ~ 2.8 ° in the 2θ scale.

3.2. Studies on small angle X-ray scattering for large q region

SAXS was also used to characterize the interface between the particles and the matrix. Porod's law indicates that in large q region (qD >> 1) the following relationship suggests the existence of sharply defined phase boundaries:

$$I(q) = \frac{K_p'}{q^4}$$

where K_p' is the Porod's constant. Such a relationship can be generalized as the power-law scattering when qD>>1:

$$I(q) \propto q^{-\alpha}$$

The power law scattering is a powerful tool to characterize the interface between two phases. For a non-fractal system, $\alpha = 4$ means a sharp interface, $\alpha = 2$ means a flake shape of the particles (pores) and $\alpha = 1$ means a rod shape. For a fractal system, α is interpreted as the fractal dimension. As shown in Figure 3(a) and (b), the scattering effect results from pores in the composite of Ni-B$_4$C and Al-SiC because the particle sizes in these composites are in the micron scale and their contribution of scattering will be smeared out. Figure 3(a) and (b) reveals that the α value approaches 4 and suggests a smooth interface. However, in Figure 3(c) there exists two regions and α was determined to be as $\alpha = 2.4$ and $\alpha = 3.3$, respectively. Figure 3(c) suggests a fractal system.
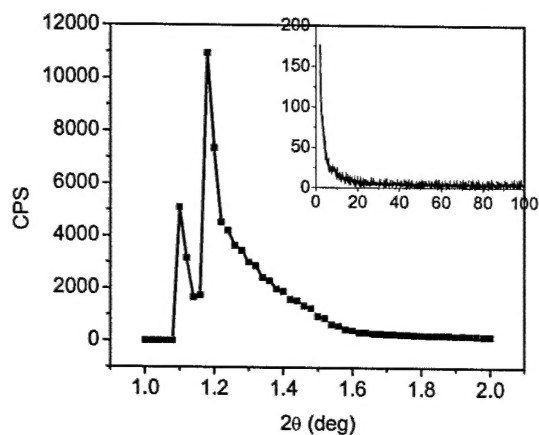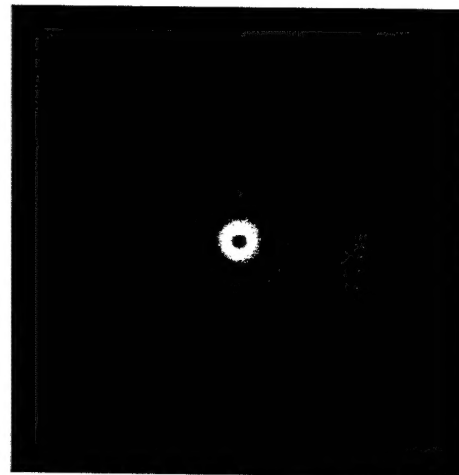

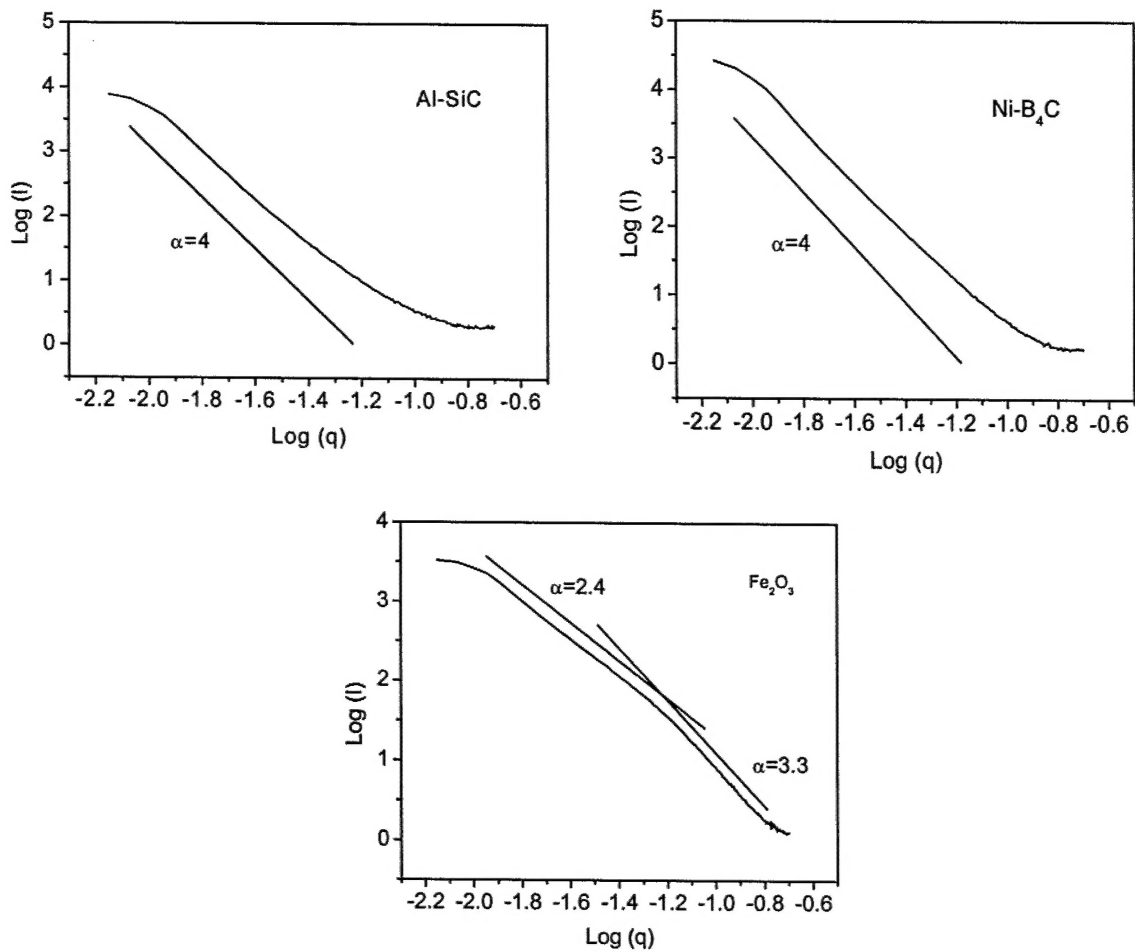Figure 2. SAXS pattern for silver behenate with (0 0 l) spacing of 58.38 Å.

Figure 3. Power law plots of log(I) vs. log(q) for (a) Al-SiC, (b) Ni-B$_4$C and (c) Fe$_2$O$_3$.

3.3. Studies on small angle scattering for small q region

In small q region (qD << 1), the Guinier's law is employed to describe the particle size in the matrix. A particle in the SAXS is defined as a volume of homogeneous electron density. In other words, the particle size is related to electronic gyration radius of the particle around its electronic center. The gyration radius can be calculated using Guinier's approximation:
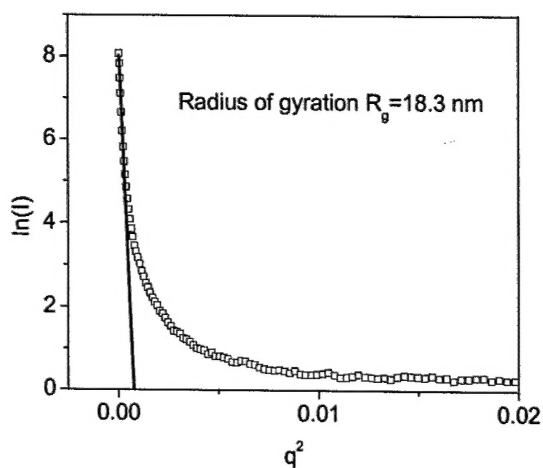
Figure 4. Guinier plot of ln(I) vs. q^2 for the partially devitrified Al$_{85}$Ni$_{10}$La$_5$ amorphous alloy annealed at 235°C for 30 min.
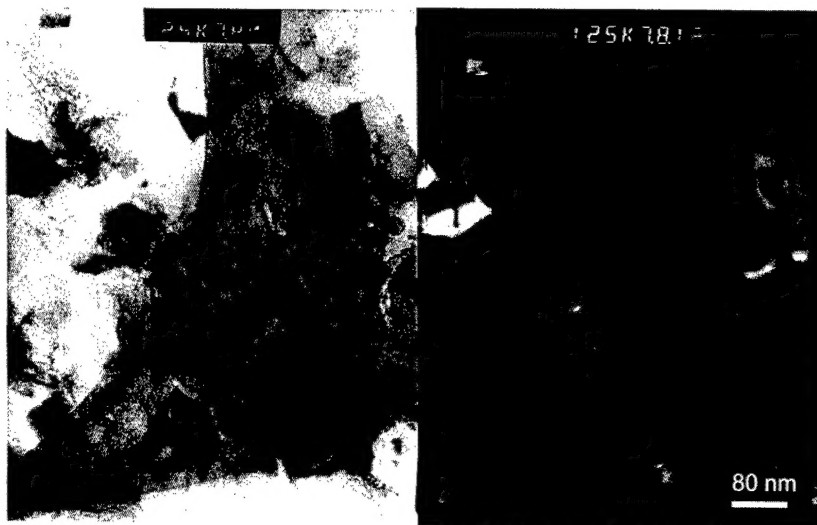

Figure 5. TEM micrographs for the partially devitrified Al$_{85}$Ni$_{10}$La$_5$ amorphous alloy annealed at 235°C for 30 min.

$$I(q) = (\Delta\rho)^2 e^{-\frac{q^2 R_g^2}{3}}$$

where $I(q)$ is the intensity. $\Delta\rho$, the difference of electron density between the particle and its neighborhood; $q = 4\pi\sin\theta/\lambda$, the wave vector; and R_g, the gyration radius.

For spherical shape, the radius of sphere is written as:

$$\langle R \rangle = \left(\frac{5}{3}\right)^{1/2} \langle R_g \rangle$$

Figure 4 shows that the Guinier's approximation can be used to determine the crystallite size of a partially crystallized amorphous $Al_{85}Ni_{10}La_5$ alloy produced by gas atomization. The amorphous powders were annealed at 235°C for 30 min and have a microstructure with aluminum crystallite precipitated out of the amorphous matrix. The radius of gyration of the crystallite is determined as $R_g = 18.3$ nm. Assuming a spherical shape, the averaged crystallite size is evaluated as 47 nm, which agrees well with the particle size determined by TEM images, as shown in Figure 5.
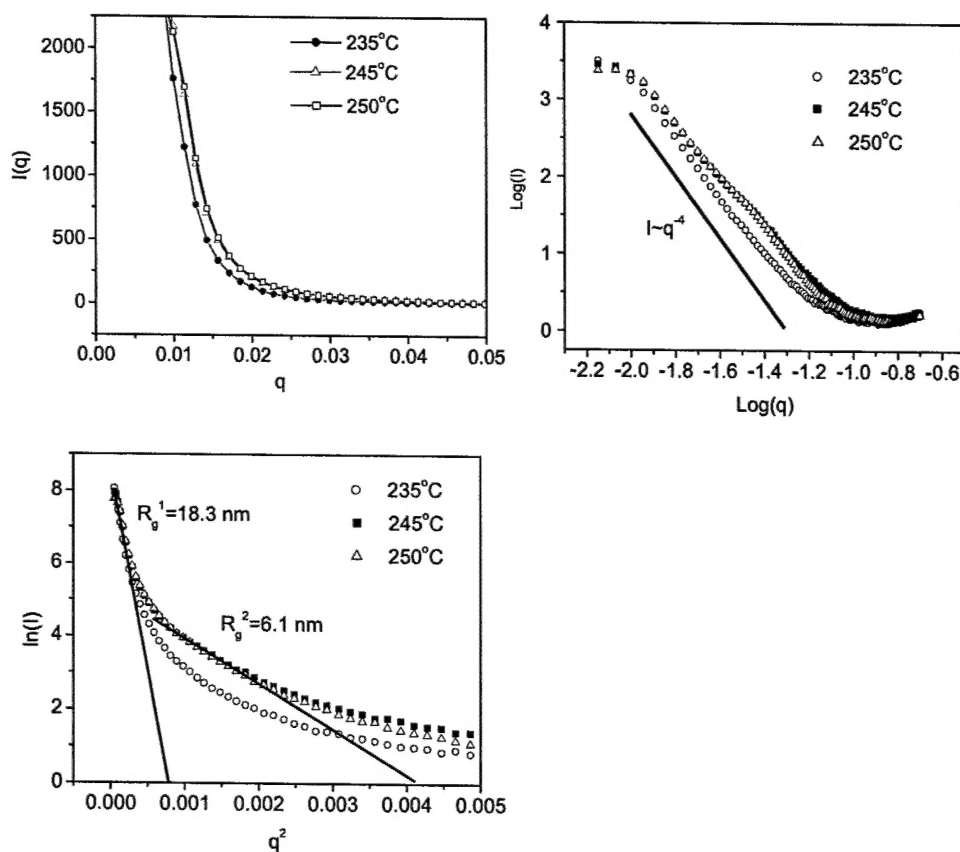

Figure 6. Isothermal DSC traces for an $Al_{85}Ni_{10}La_5$ amorphous alloy annealed for 30 min at 235°C, 245°C and 250°C respectively.

Figure 7. SAXS scattering patterns for an $Al_{85}Ni_{10}La_5$ amorphous alloy annealed for 30 min at 235°C, 245°C and 250°C respectively. (a) I vs. q plot, (b) log(I) vs. log(q) plot and (c) ln(I) vs. q² plot.

Figure 8. TEM dark field image for the partially devitrified $Al_{85}Ni_{10}La_5$ amorphous alloy annealed at 245°C for 30 min.

3.4 Studies on crystallization behavior of an amorphous $Al_{85}Ni_{10}La_5$ alloy using SAXS

The crystallization behavior of an amorphous $Al_{85}Ni_{10}La_5$ alloy was studied using SAXS. Fully amorphous powders (< 25 μm) were produced by gas atomization and the XRD pattern exhibits a diffusive hump and no sharp peak occurs. The amorphous powders were annealed for 30 min at 235°C, 245°C and 250°C respectively, as shown in Figure 6. The observance of a
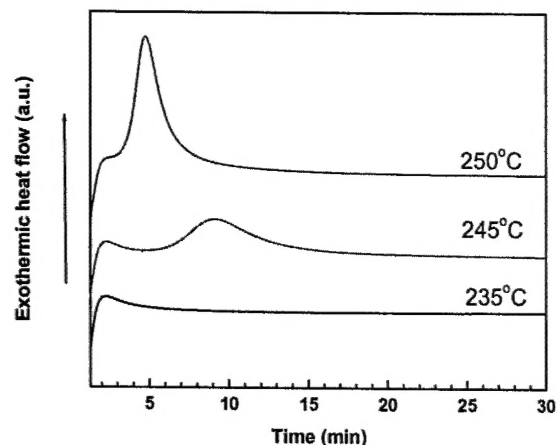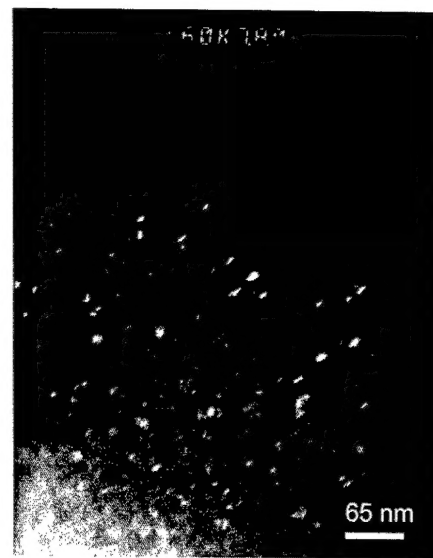
monotonically decreasing signal suggested a grain growth behavior in the isothermal DSC traces performed at 235°C, indicating that the crystallization at 235°C results from the growth of quenched-in aluminum nuclei. On the contrary, observance of an exothermic peak suggested a nucleation and growth behavior in the isothermal DSC tracing at 245°C and 250°C.

Figure 7(a) shows the SAXS patterns for the amorphous powders after annealed at 235°C, 245°C and 250°C respectively. It is seen that the scattering intensity for the powders annealed at 245°C and 250°C is similar but higher than that for 235°C, indicating a considerable increase of scatterers at the temperatures above 235°C, suggesting that more crystallite precipitated from the matrix. Figure 7(b) shows the logarithmic power-law plots for the annealed amorphous powders. The slope approaching – 4 indicates that a sharp interface exists between the particles and matrix. Again, this result supports that the crystallization is a thermally activated process instead of the spinodal decomposition process. A careful observation of the patterns for 245°C and 250°C in Figure 7(b) further revealed that the signals may result from two sets of particles with different size. This estimation was confirmed in Figure 7(c). In the Guinier's plot of ln(I) vs. q^2, one can see two regions that fit the Guinier's approximation. The gyration of radii are determined as $R_g^1 = 18.3$ nm and $R_g^2 = 6.1$ nm, corresponding to an averaged particle size of 47 nm and 16 nm, respectively. The presence of a smaller particle sized region can be observed in TEM, as shown in Figure 8.

3.5 Studies on interface between ceramic and metal using SAXS

Experiments were conducted to determine the inherent nature of the interface in the powder particles of Al/SiC and Ni/B$_4$C. SiC and B$_4$C were coated with the respective metals (Al and Ni) in a fluid-bed batch-manufacturing process. SAXS is deployed to determine the shape and size of nano-voids at the interfaces between ceramic and metal. The nature of the surfaces was examined too.

Least-square curve fitting was first performed on the scattering intensity using Mathematica. The model was based on the equation of $I(h) = A + \dfrac{B}{C + Exp(h) - Exp(-h)}$ where $h = q^2 = (4\pi \dfrac{\sin\theta}{\lambda})^2$. A and B are parameters that are refined in the regression. Radius of gyration, R_g was then determined via the Guinier Equation: $LnI(h) = q^2 \dfrac{4\pi^2}{3\lambda^2} R_o^2 + const$. By the strictest rule, R_g is determined at the slope of the curve $I(h^2)$ when h=0; this was adhered in this experiment. A normal distribution was assumed for the particle size distribution of these voids. The scattered intensity could then be modeled as

$$I(h) = NV(\rho - \rho_o) \int_0^\infty (\frac{\pi d^3}{6})^2 f(d) P(h,d)\delta d \quad \text{where} \quad f(d) = \frac{1}{\sigma\sqrt{2\pi}} Exp\left\{-\frac{(d - d_{50})^2}{8\sigma^2}\right\} \quad \text{and} \quad d_{50} = 2R_{50} = \sqrt{\frac{5}{3}}R_g.$$

The scattered intensity was re-plotted on a Ln-Ln scale to determine the α factor as in the $<|F(q)|^2 >= F_o q^{-\alpha}$ where $I(q) = I_e |F(q)|^2$, I$_e$ is the Thomson scattering from one electron, and F$_0$ is a constant. The parameter of α describes the nature of the interface (as discussed before); the interface is smooth when α=4 (non-fractal scatterer with a Euclidean dimension=3 (3-D space)), $3 < \alpha \leq 4$ for surface fractal, $\alpha < 3$ for mass fractal. A α value of 2 and 1 could also mean thin plane lamina and thin rod shapes, respectively if the scatterers are non-fractal. It should be highlighted that R_g is derived from the gradient of the scattering intensity curve at the q=0 whereas α is determined at higher immediate q values.

Table 1. The Radius of gyration, R_g and R_{50} of the nano-voids in the MMCs

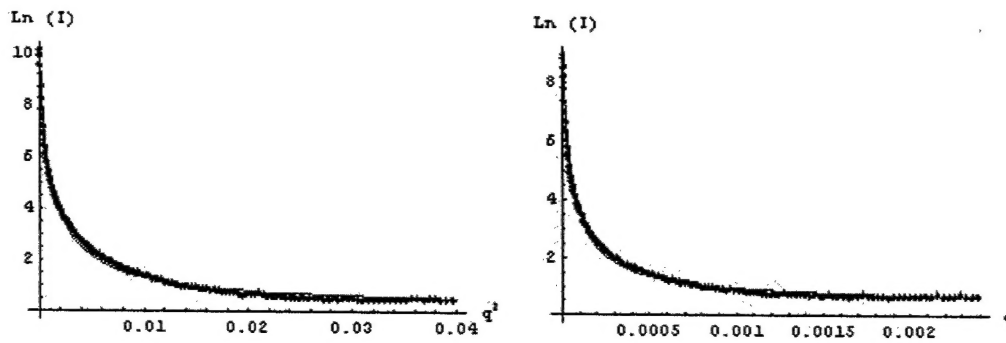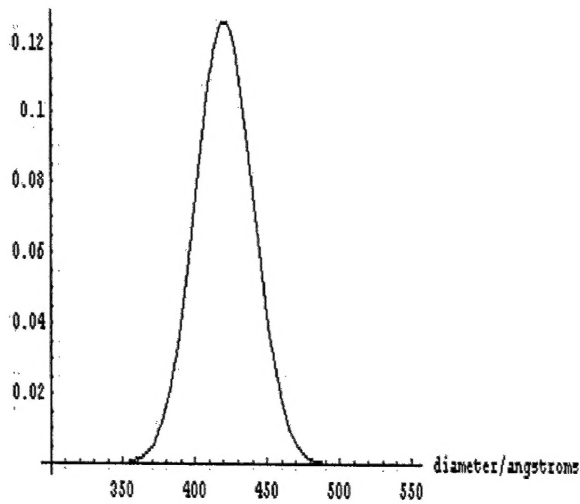| Material	Radius of gyration, R_g	Radius, R_{50}
Al/SiC	148.691	210.3
Ni/B$_4$C	165.691	427.812

Figure 9. Ni/B₄C (Left) and Al/SiC (Right) are illustrations which reflected the accuracy of the curve fitting model (the red lines denote the fitted curve) from which the radius of gyration, R_g is determined.
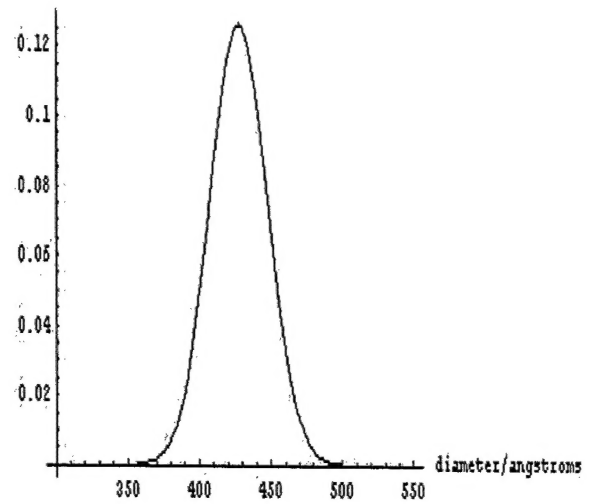

Figure 10. Nano-voids size distribution in Ni/B₄C MMC powder particles (Left); Nano-voids size distribution in Al/SiC MMC powder particles (Right).

The R_{50} is determined from the R_g assuming the voids possessed nearly spherical shape (Table 1). The model, $I(h) = A + \dfrac{B}{C + Exp(h) - Exp(-h)}$ was manifested as a fairly accurate fit to the scattered intensities as shown in Figure 9(a) and (b). The normal distribution of these voids are then modeled, as shown in Figure 10(a) and Figure 10(b). From the graphs, there is a slightly larger size variation of the nano-voids in Al/SiC than in Ni/B₄C. The limiting factor in the nano-voids size and its distribution determination could possibly lie in the process than the materials involved.

From the intermediate values of q (Figure 11(a) and Figure 11(b)), α is determined from the gradient of the slope to be 3.61 and 3.75 in Ni/B₄C and Al/SiC respectively. Therefore, both are surface fractals; i.e. the surfaces of nano-voids are not smooth. Although α does not serve as a physical tangible value, $\Delta\alpha$ could aid in the understanding of the evolution of the nano-voids in subsequent processing or consolidation of these powder particles.
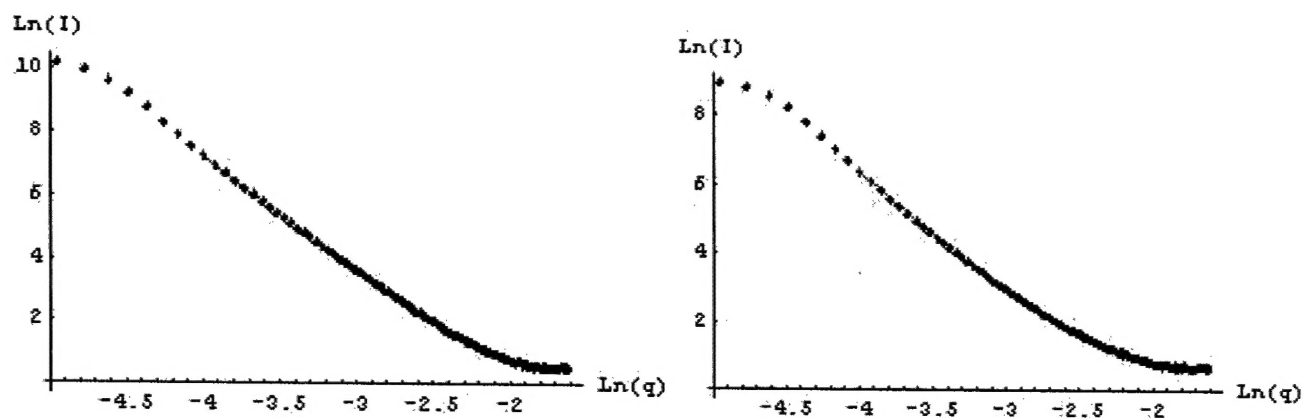
Figure 11. Fractal determination $<|F(q)|^2 >= F_o q^{-\alpha}$ in Ni/B$_4$C MMC powder particles (Left); Fractal determination $<|F(q)|^2 >= F_o q^{-\alpha}$ in Al/SiC MMC powder particles (Right). The red line denotes the power-law scattering model.

4. References

1. A. Guinier, G. Fournet, Small Angle Scattering of X-rays, John Wiley& Sons, Inc., 1955
2. P.W. Schmidt, Some Fundamental Concepts and Techniques useful in Small-Angle Scattering Studies or Disordered Solids, H. Brumberger (ed.) Modern Aspects of Small-Angle Scattering, 1-56
3. L.J. Effler, J.F. Fellers, J.S. Lin, Small Angle X-ray Scattering Behavior of Mircoporous Fiber used in Composite Structures, T.L. Vigo and B.J. kinzig (ed.) Composite Applications-The role of Matrix, Fiber and Interface, 179-207
4. K. Nakamura, T. Kawabata, Y. Mori, Powder Technology 131 (2003) 120-128